

## Prediction of Tornadoes and Typhoons (Hurricanes) by Using Gravity Wave Diagnostics\*

R. J. HUNG

*The University of Alabama in Huntsville  
Huntsville, Alabama 35807 U. S. A.*

(Manuscript received 18 January, 1977, in revised form 19 March, 1977)

### ABSTRACT

Ground-based ionospheric sounding array observed gravity waves with wave periods of 13 to 28 minutes (mostly around 13 minutes) and with horizontal phase velocities of 90 to 220 m/sec during tornadic storms, and gravity waves with wave periods of 21 to 25 minutes, and with horizontal phase velocities of 110 to 210 m/sec during hurricanes at the *F*-region ionospheric height. By using data on the neutral atmosphere and neutral wind profiles, a group ray tracing computation has been carried out in an attempt to locate the sources of these waves. By comparing the results of the computed sources of the waves and the actual location and time of the tornado touchdown, it is found that the location of tornado touchdown was within 50 km distance from the computed location of the sources of waves, and the signals excited by storms were 2 to 4 hours ahead of the touchdown of tornadoes of the present study. For the case of hurricanes, it was found that the computed locations of the source were located along the storm track 3 to 4 hours ahead of the actual location of the eye wall. The nature of the applicability of the present study to a severe storm warning system is discussed.

### 1. Introduction

Upper atmospheric wave-like disturbances at ionospheric heights are frequently observed on ground-based ionospheric sounding records as perturbations in the electron densities. Observations made by Georges (1968), Baker and Davies (1969), Davies and Jones (1972), Hung, *et al.* (1975), and Smith and Hung (1975) show a correlation between ionospheric wave-like disturbances and severe weather activity. However, the identification of the sources of these waves has always been a difficult problem.

In this study we have employed a continuous wave-spectrum high frequency Doppler sounder array to observe the dynamics of the upper atmospheric disturbances during the tornadic storms and hurricanes. The event

chosen for the tornadic storms was the extreme tornado out-break of April 3, 1974; and for hurricanes, was Hurricane Eloise during the period September 22-23, 1975. The evidence for the coupling of energy from the troposphere into the ionosphere has come from observations of electron density fluctuations which appear as changes of phase and frequency of the ionospherically reflected radio waves. In this study, we have used a technique whereby radio receivers located at a central site will monitor signals transmitted from three independent remote sites and reflected off the ionosphere approximately half way between the transmitter and the receiver sites. When an electron density profile in the ionosphere is disturbed and fluctuated, the total phase path  $P$  of the radio signal changes; and the instantaneous frequency shift  $\Delta f$  of a radio echo of frequency  $f$  is given by

$$\Delta f = - \frac{f}{c} \frac{dp}{dt} \quad (1-1)$$

\* This paper was presented at the National Taiwan University, December 1976, sponsored by the Department of Atmospheric Sciences, National Taiwan University and the Chinese Meteorological Society.

where

$$p = \int \mu \cos \alpha ds \quad (1-2)$$

Here  $c$  is the speed of light;  $\mu$ , the real part of the refractive index;  $\alpha$ , the angle between the wave normal and the ray;  $ds$ , the element of the ray path  $s$ . Tropospheric disturbances provide unique structure variations in the refractive index modified by infrasonic-gravity waves which are readily detectable by this technique.

Analysis of the Doppler records of the ionospheric fluctuations during the time period of the tornado outbreak of April 3, 1974, indicates that gravity waves with wave periods in the range of 13 to 28 minutes (mostly around 13 minutes) and the horizontal phase velocities of 90 to 220 m/sec were observed. For the case of the analysis of Doppler data during Hurricane Eloise on September 22-23, 1975, it was found that gravity waves with wave periods in the range of 21 to 25 minutes and the horizontal phase velocities of 110 to 210 m/sec were detected. Since the local buoyancy frequency at  $F$ -region ionospheric height (say, 200 km altitude) is 10 minutes and the wave periods observed is longer than the local buoyancy frequency, the ionospheric disturbances associated with tornadic storms and hurricanes belong to the category of gravity waves.

The identification of the sources of waves has been attempted. With the consideration of background wind and the data on neutral atmosphere from the ground to the ionospheric height, a reverse ray tracing computation was accomplished. The computed location of the probable sources of waves were within 50 km distance from the location of the actual touchdown of the tornadoes. Furthermore, it was discovered that the signals excited by the tornadic storms were 2 to 4 hours ahead of the touchdown of the tornadoes. On the other hand, for the computation of waves associated with the hurricane, it was found that the computed locations of the source were located along the storm track 3 to 4 hours ahead of the actual location of the eye wall. The techniques used in the present analysis and also the results obtained could be significant in the future development of the severe storm warning systems.

## 2. Experimental Arrangements and Procedure

Our Doppler sounder array system consists of three sites with nine field transmitters operating at 4.0125, 4.759 and 5.734 MHz. These sites are located at Ft. McClellan, Alabama (33°44'N, and 85°48'W); TVA, Muscle Shoals, Alabama (34°46'N, and 85°38'W); and TVA, Nickajack Dam, Tennessee (35°01'N and 87°38'W); with receivers located at NASA/Marshall Space Flight Center, Alabama (34°39'N and 86°40'W). Since each of three transmitters uses the same nominal frequency, the actual frequencies must be slightly different so that they can be distinguished from each other at the receiver. At the receiving station, the oscillators have been set exactly at the nominal frequencies, so that in the absence of Doppler variations, the offsets of the transmitter oscillators are equal to the beat frequencies.

(A) **Tornadic Storms.** During the extreme tornado outbreak of April 3, 1974, we observed wave-like fluctuations other than the ordinary traveling ionospheric disturbances (TID's). Doppler records observed were subjected to power spectral density analysis and cross correlation analysis (Appendix A). It was found that correlation was very poor for the signals detected before 1700 UT. Figs. 1, 2 and 3 show power spectral density of ionospheric disturbances from the transmitters at Muscle Shoals, Alabama; Ft. McClellan, Alabama; and Nickajack Dam, Tennessee, to the receivers at Huntsville, Alabama, respectively, at the observation time 1700-1800 UT, April 3, 1974. The average wave period of the disturbances during 1700-1800 UT is 13 minutes. Figures for the power spectral density of ionospheric disturbances during the other time period of observation will be omitted in this paper. The average wave periods of the disturbances at the observation times 1800-1900 UT, 1900-2000 UT, and 2000-2200 UT, April 3, 1974, are 13 minutes, 13.5 minutes, and 28 minutes, respectively. For the observation time 2200-2400 UT, TID's were detected, and the results will be given elsewhere. After 2400 UT, correlation was very poor for the signals detected.

The horizontal phase velocity of the disturbances can be calculated from cross-correlograms. This is because the zero frequency

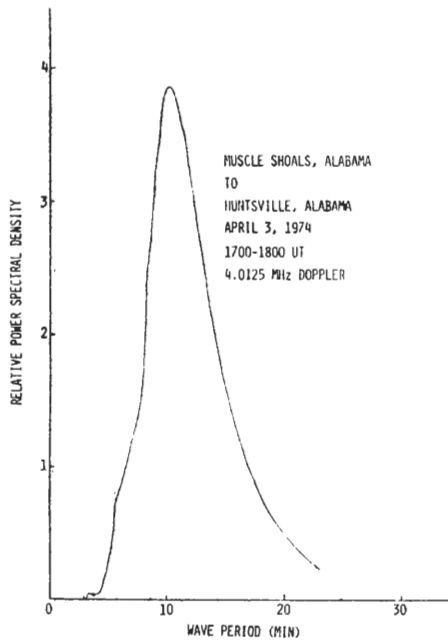


Fig. 1. Power spectral density of ionospheric disturbances from Muscle Shoals, Ala. to Huntsville, Ala., at 1700-1800 UT, April 3, 1974, at the operating frequency 4.0125 MHz.

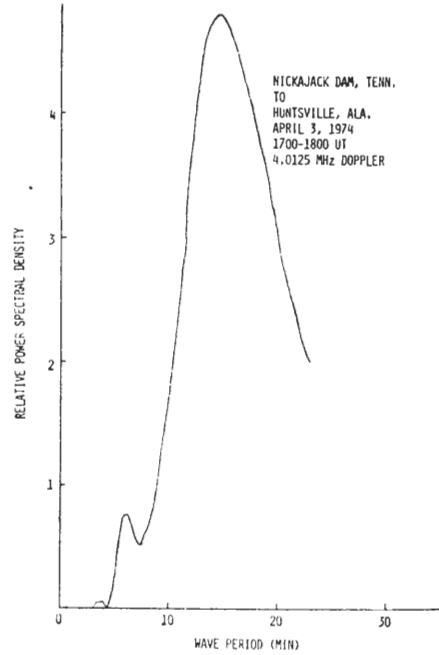


Fig. 3. Power spectral density of ionospheric disturbances from Nickajack Dam, Tenn. to Huntsville, Ala., at 1700-1800 UT, April 3, 1974, at the operating frequency 4.012 MHz.

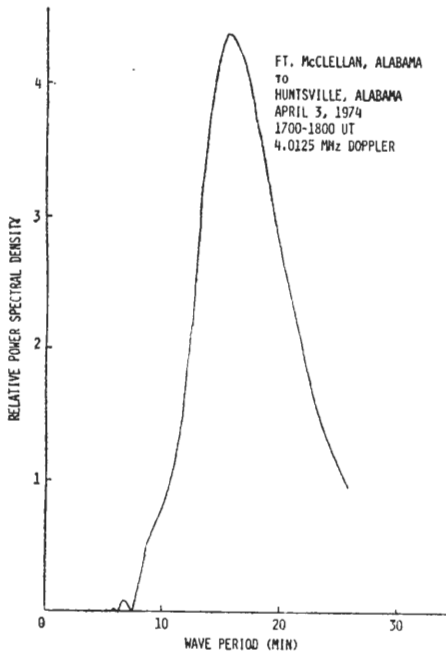


Fig. 2. Power spectral density of ionospheric disturbances from Ft. McClellan, Ala. to Huntsville, Ala., at 1700-1800 UT, April 3, 1974, at the operating frequency 4.0125 MHz.

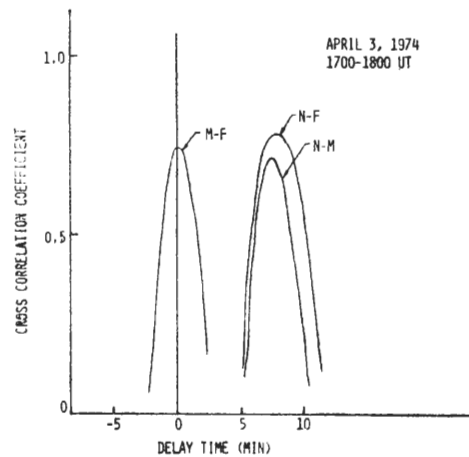


Fig. 4. Cross-correlograms from Nickajack Dam (N), Muscle Shoals (M), and Ft. McClellan (F) at time period 1700-1900 UT, April 3, 1974.

crossings are essentially independent of the amplitude of the change of height of the reflecting surface and they can be used to determine the average period and average time displacement (Davies and Jones, 1972). Fig. 4 shows cross-correlograms during the time interval 1700-1800 UT, April 3, 1974. The acceptable combinations of time displacement,  $\Delta t$ , between the signals detected at the two ionospheric reflection points must satisfy the relationship,

$$(\Delta t)_{F-M} + (\Delta t)_{M-N} = (\Delta t)_{F-N} \quad (2-1)$$

where the subscript  $F-M$  denotes the time delay between Ft. McClellan and Muscle Shoals; subscript  $M-N$ , the time delay between Muscle Shoals and Nickajack Dam; and subscript  $F-N$ , the time delay between Ft. McClellan and Nickajack Dam. The cross-correlograms given in Fig. 4 clearly indicates that the relationship (2-1) is satisfied.

In this experiment, the following information was obtained: (1) in the time period 1700-1800 UT, gravity waves with wave periods of 13 minutes, azimuthal angle of the wave vector  $220^\circ$ , and horizontal phase speed 133 m/sec were observed; (2) in the time period 1800-1900 UT, gravity waves with wave periods of 13 minutes, azimuthal angle of the wave vector  $255^\circ$ , and horizontal phase speed 217 m/sec were detected; (3) in the time period 1900-2000 UT, gravity waves with wave periods of 13.5 minutes, azimuthal angle of the wave vector  $146^\circ$ , and horizontal phase speed 160 m/sec were detected; and (4) in the time period 2000-2200 UT, gravity waves with wave periods of 28 minutes, azimuthal angle of wave vector  $179^\circ$ , and horizontal phase speed 90 m/sec were observed.

(B) **Hurricane.** During the time periods of Hurricane Eloise activity on September 22-23, 1975, wave-like fluctuations were observed at  $F$ -region ionospheric height. Similar to the procedures which we mentioned above, Doppler records observed were subjected to power spectral density analysis and cross correlation analysis. Figs. 5, 6 and 7 show power spectral density of the ionospheric disturbances from the transmitters at Muscle Shoals, Alabama; Ft. McClellan, Alabama; and Nickajack Dam, Tennessee, to the receivers in Huntsville, Alabama, respectively, at the observation time 0200-0340 UT, September 23, 1975. The average wave period of the disturbances during 0200-

0340 UT is 22 minutes. At another observation time, 0500-0730 UT, September 23, 1975, the average wave period of the disturbances is also 22 minutes.

As usual, the horizontal phase velocity of the disturbances can be computed from cross correlograms. Fig. 8 shows cross correlograms during the time interval 0200-0340 UT, September 23, 1975. The phase velocity obtained in this observation period is 195 m/sec. The similar computation applied to the observation period 0500-0730 UT, 1975 is 200 m/sec.

Results obtained from the experiments are then subjected to a reverse ray tracing computation by using data on the neutral atmosphere and wind profiles, and an attempt is made to locate the sources of these waves. A detailed description will be given in the following sections.

### 3. Ray Path Computation

The characteristics of acoustic-gravity waves are described by the dispersion relation which for an isothermal atmosphere has the form (Hines, 1960):

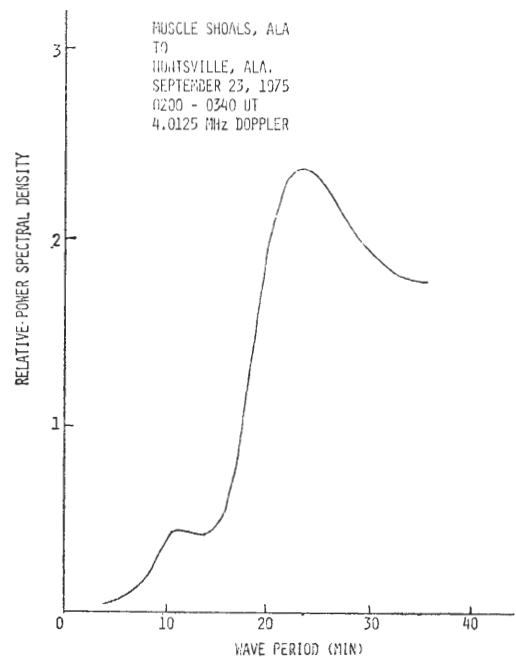


Fig. 5. Power spectral density of ionospheric disturbances from Muscle Shoals, Ala. to Huntsville, Ala., at 0200-0340 UT, September 23, 1975, at the operating frequency 4.0125 MHz.

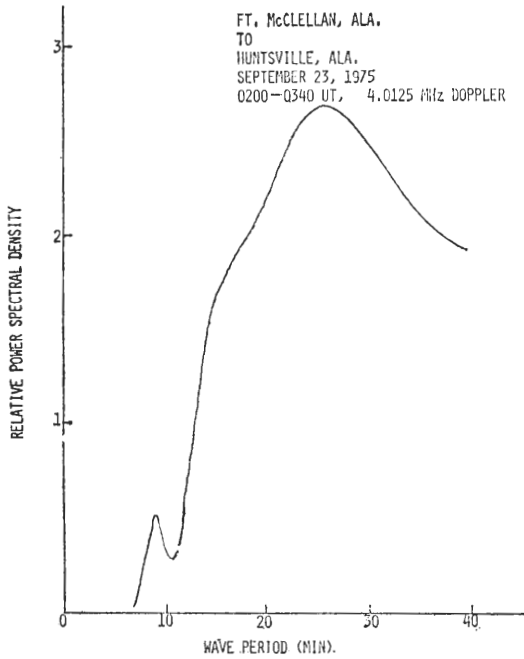


Fig. 6. Power spectral density of ionospheric disturbances from Ft. McClellan, Ala. to Huntsville, Ala., at 0200-0340 UT, September 23, 1975, at the operating frequency 4.0125 MHz.

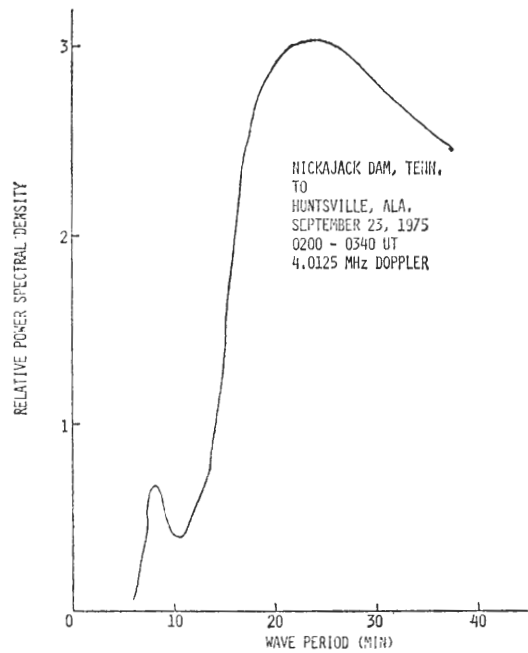


Fig. 7. Power spectral density of ionospheric disturbances from Nickajack Dam, Tenn. to Huntsville, Ala., at 0200-0340 UT, September 23, 1975, at the operating frequency 4.0125 MHz.

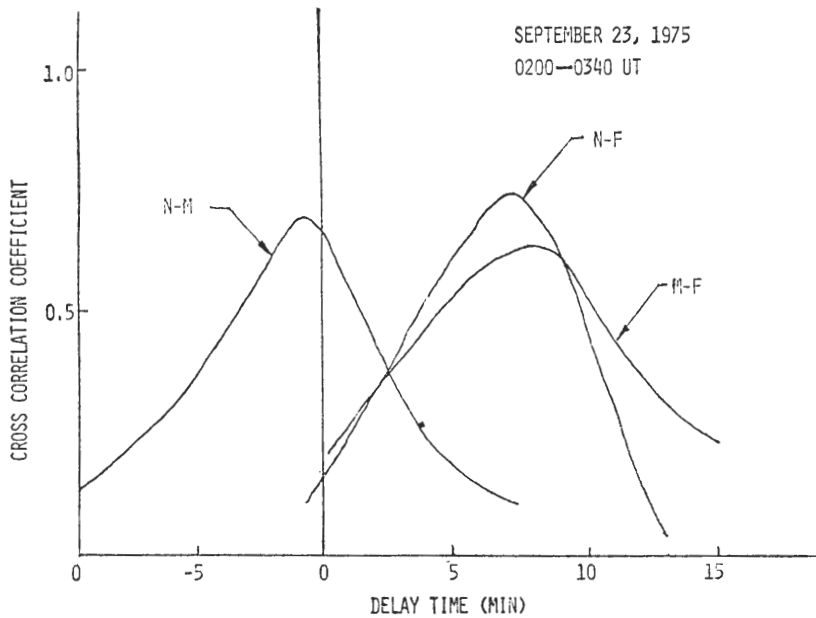


Fig. 8. Cross-correlograms from Nickajack Dam (N), Muscle Shoals (M), and Ft. McClellan (F) at time period 0200-0340 UT, September 23, 1975.

$\omega^4 - \omega^2 c^2 (k_x^2 + k_z^2) + g^2 (\gamma - 1) k_x^2 + i \omega^2 \gamma g k_x = 0$  (3-1)  
 where  $\omega$  denotes wave frequency;  $k_x$ , the horizontal wave number;  $k_z$ , the vertical wave number;  $c$ , the velocity of sound;  $\gamma$ , the ratio of specific heat; and  $g$ , the acceleration due to gravity. Equation (3-1) is complex even for the lossless medium. The choice of real or complex  $\omega$ ,  $k_x$  and  $k_z$  depends on the problem of interest. For example, if the problem of interest is concerned with imperfect horizontal ducting,  $k_x$  may become complex number to show leakage of energy from the duct. In the present problem, we have considered waves to be incident on a horizontally stratified medium. Due to the kinematic boundary conditions at interfaces,  $k_x$  must be invariant from stratification to stratification and is therefore real.  $\omega$  is real for the case of forced oscillation. Thus,  $k_z$  must be complex since  $\omega$  and  $k_x$  are real. Let

$$k_z = k_z^r + i k_z^i \tag{3-2}$$

where  $k_z^r$  is the real component and  $k_z^i$  is the imaginary component of  $k_z$ . The real part and imaginary part of Equation (3-1) can be easily separated to give the following two equations:

$$\omega^4 - \omega^2 c^2 (k_x^2 + k_z^{r2} - k_z^{i2}) + g^2 (\gamma - 1) k_x^2 - \omega^2 \gamma g k_z^i = 0 \tag{3-3}$$

$$\omega^2 k_z^i (2c^2 k_z^i - \gamma g) = 0 \tag{3-4}$$

If  $k_z^r \neq 0$  so that there is a phase variation along the vertical height,  $z$ , then, from Equation (3-4),  $k_z^i$  must be a constant given by

$$k_z^i = \frac{\gamma g}{2c^2} \tag{3-5}$$

Substituting Equation (3-5) by Equation (3-3) yields

$$\left(1 - \frac{\omega_a^2}{\omega^2}\right)^{-1} \left[ k_x^2 \left(1 - \frac{\omega_b^2}{\omega^2}\right) + k_z^{r2} \right] = \frac{\omega^2}{c^2} \tag{3-6}$$

where  $\omega_a = \gamma g / 2c$  is the acoustic cutoff frequency, and  $\omega_b = (\gamma - 1)^{1/2} g / c$  is the buoyancy frequency. In an isothermal atmosphere, we have  $\omega_a > \omega_b$  since  $\gamma$  is less than 2. It is interesting to discuss the properties of the dispersion relation, Equation (3-6), in three different frequency ranges. (1) For  $\omega > \omega_a > \omega_b$ , Equation (3-6) becomes ellipse, and the waves in this region are generally termed as acoustic waves; (2) For  $\omega_a > \omega > \omega_b$ , either  $k_x$  or  $k_z^r$  has to be imaginary, contrary to the initial assumption, and this

region is known as the cutoff region; and (3) For  $\omega_a > \omega_b > \omega$ , Equation (3-6) becomes hyperbola, and the waves in this region are termed as gravity waves. In the real atmosphere, the buoyancy frequency is given by

$$\omega_b = \left[ -g \left( \frac{d \ln \rho}{dz} + \frac{g}{c^2} \right) \right]^{1/2} = \left[ \frac{(\gamma - 1)g^2}{c^2} + \frac{g}{c^2} \frac{dc^2}{dz} \right]^{1/2} \tag{3-7}$$

which may become greater than  $\omega_a$ , where  $\rho$  is the density of the medium. Thus, in the real atmosphere, the cutoff region of the form discussed for isothermal atmosphere no longer exists.

The location of the source of the wave generating mechanism can be computed by using the technique of triangulation from the cross-correlations calculated from the Doppler records obtained from the three sites (three different locations with distances 94, 95 and 134 km apart from each other) and nine transmitters (reflected from three different altitudes), if the background wind velocity is much less than the group velocity of the infrasonic-gravity waves observed during periods of severe storms and medium is homogeneous. If the wind velocity is comparable to the group velocity of the waves and the background medium is inhomogeneous, a ray tracing analysis becomes necessary. Theoretical discussions of group rays of infrasonic-gravity waves have been carried out by Bretherton (1966), Jones (1969), Cowling, *et al.* (1971) and Bertin, *et al.* (1975). These discussions indicate that the geometrical optics approximation seems valid under the conditions discussed. The wave propagated is assumed to be locally plane so that a local dispersion relation, Equation (3-6), is satisfied. Ray tracing, thus, could be carried out by following the group velocity direction in a wind-stratified model atmosphere.

The effect of the wind can be taken into account by considering the time-space transformation given by Galilean transformation

$$\left. \begin{aligned} \mathbf{r}' &= \mathbf{r} - \mathbf{u}t, & t' &= t \\ \omega' &= \omega - \mathbf{k} \cdot \mathbf{u}, & \mathbf{k}' &= \mathbf{k} \end{aligned} \right\} \tag{3-8}$$

where  $\mathbf{r}$  and  $t$  denote the displacement vector and time, respectively. All quantities expressed in unprimed form are observed in the stationary coordinate system, and those in primed form are

in the coordinate system moving with the medium with a constant horizontal velocity  $\mathbf{u}$ . To compute a wave package incident from below into a horizontally stratified atmosphere in the presence of horizontal wind shear, we can assume that the medium can be thought of as being made up of horizontally stratified layers. In each layer, a dispersion relation, Equation (3-6), is satisfied. The kinematic boundary condition requires that the horizontal wave vector be matched from layer to layer, i. e.,

$$(\mathbf{k}_x)_i' = (\mathbf{k}_x)_0' = \mathbf{k}_x \quad (3-9)$$

where  $(\mathbf{k}_x)_0'$  is horizontal wave number at incidence and  $(\mathbf{k}_x)_i'$  is that in the  $i$ th layer,  $i=1, 2, 3, \dots$ . This condition, Equation (3-9), together with the Galilian transformation, Equation (3-8), indicates that the horizontal wavelength shall be constant while the wave frequency is shifted in the presence of background wind when the wave propagates from the stratosphere up to the ionosphere.

It is known that, in a lossless, transparent medium, energy propagates along the direction of the group velocity,  $\mathbf{v}_g$  (e. g., Yeh and Liu, 1972). This direction is termed the ray direction. In general in an anisotropic medium the ray direction is different from that of the wave vector  $\mathbf{k}$ . The definition of group velocity is

$$\mathbf{v}_g = \nabla_{\mathbf{k}} \omega(\mathbf{k}) \quad (3-10)$$

It is obvious that  $\mathbf{v}_g$  is normal to the surface  $\omega(\mathbf{k}) = \text{constant}$  which is the solution of the dispersion relation, Equation (3-6) for atmospheric waves, with a fixed frequency. For the presence of horizontal wind, with the substitution of Equations (3-6), (3-8) and (3-9) in Equation (3-10), the expressions for the group velocity of the waves in the moving frame of reference yield

$$v_{gz} = - \frac{c^2 \omega' k_z'}{c^2(k_x^2 + k_z'^2) - 2\omega'^2 + \omega_a^2} \quad (3-11)$$

$$v_{gx} = \frac{(\omega_b^2 - \omega'^2) c^2 k_x}{[c^2(k_x^2 + k_z'^2) - 2\omega'^2 + \omega_a^2] \omega'} \quad (3-12)$$

where the superscript  $r$  of  $k_z'$  has been omitted. In the stationary frame, the corresponding group velocity then becomes

$$v_{gx} = v_{gx}' \quad (3-13)$$

$$\mathbf{v}_{gx} = \mathbf{v}_{gx}' + \mathbf{u} \quad (3-14)$$

The group ray in  $\mathbf{r}$ -space is possible to compute

by integrating

$$\frac{d\mathbf{r}}{dt} = \mathbf{v}_g \quad (3-15)$$

which is the group ray trajectory of the waves. Thus,  $\omega$  and  $\mathbf{k}$  propagate with  $\mathbf{v}_g$ , while the phase front propagates with  $\omega/\mathbf{k}$ .

In this computation, the neutral wind is treated as constant in each slab of the atmosphere considered. The values of  $\omega_a$ ,  $\omega_b$  and  $c$  are calculated for each altitude from the parameters of neutral atmosphere based on the U. S. Standard Atmosphere (1962). The profiles of the neutral winds are formed using data from the following two sources: (1) wind profiles above 100 km altitude are computed from the atmospheric wind model proposed by Kohl and King (1967); (2) at an altitude below 90 km, wind profiles were obtained from meteorological rocketsonde data at Cape Kennedy, Florida. Fig. 9 shows a computed vertical wind profile from the wind model for the zonal component (East-West direction) at 1200 local time or 1700 UT, April 1974. Fig. 10 shows a computed vertical wind profile of the meridional component (North-South direction) from the wind model at 1200 local time or 1700 UT, April 1974. Similarly, Figs. 11 and 12 show the computed vertical wind profiles for zonal component and meridional component, respectively, from a wind model at 1700 local time or 2200 UT, April 1974. Fig. 13 indicates an observed vertical wind profile of zonal component from meteorological rocketsonde data at 1700 UT, April 3, 1974, at Cape Kennedy, Florida. Fig. 14 shows a similarly observed vertical wind profile of meridional component from meteorological rocketsonde data at the same time and the same location. Similarly, Fig. 15 shows meridional component and zonal component of vertical wind profiles from the wind model at 0100 local time, September 1975; and Fig. 16 shows observed vertical wind profiles of meridional and zonal components from the meteorological rocketsonde data at 1426 UT, September 24, 1975, at Cape Kennedy, Florida.

The results for the reverse ray path computations and comparison with the location and time of the tornado touchdown and the storm track of the hurricane are discussed more fully in the next section.

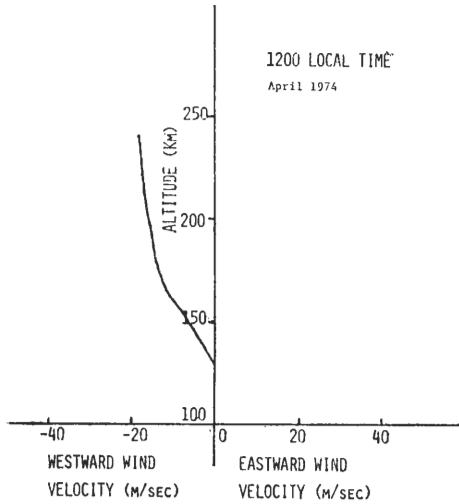


Fig. 9. Computed vertical wind profile of the zonal component (East-West direction) at 1200 local time April 1974, and 35 N latitude.

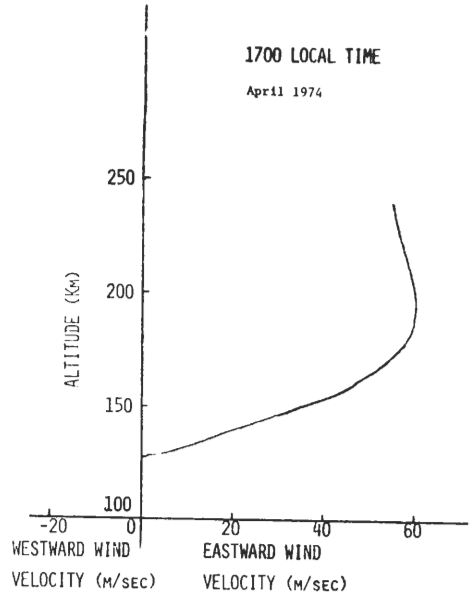


Fig. 11. Computed vertical wind profile of the zonal component (East-West direction) at 1700 local time April 1974, and 35 N latitude.

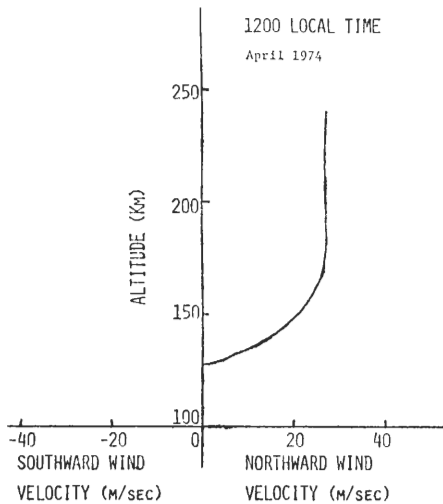


Fig. 10. Computed vertical wind profile of the meridional component (North-South direction) at 1200 local time April 1974, and 35 N latitude.

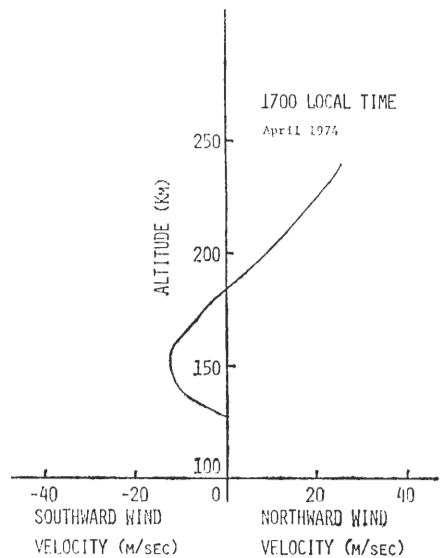


Fig. 12. Computed vertical wind profile of the meridional component (North-South direction) at 1700 local time April 1974, and 35 N latitude.



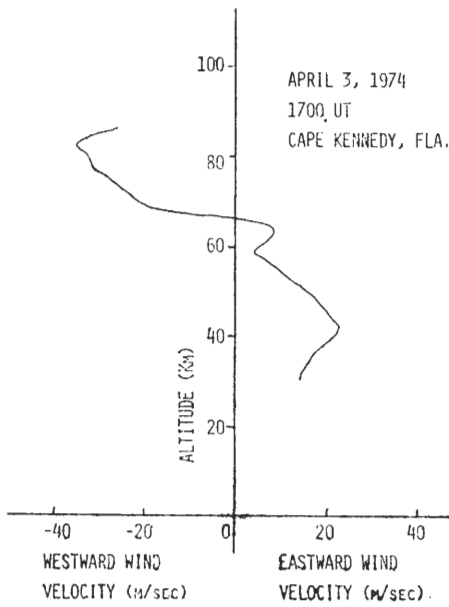


Fig. 13. Observed vertical wind profile of the zonal component (East-West direction) at 1700 UT, April 3, 1974, Cape Kennedy, Florida, based on meteorological rocketsonde data.

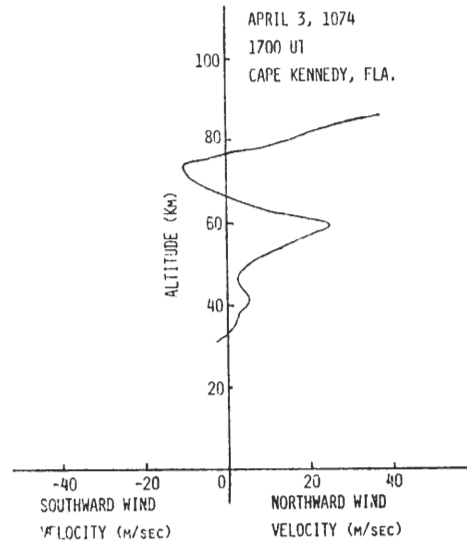


Fig. 14. Observed vertical wind profile of the meridional component (North-South direction) at 1700 UT, April 3, 1974, Cape Kennedy, Florida, based on meteorological rocketsonde data.

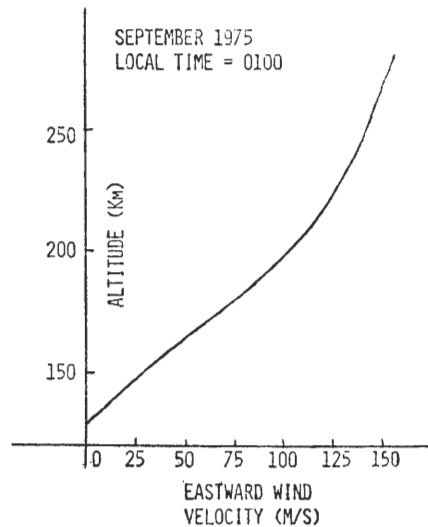
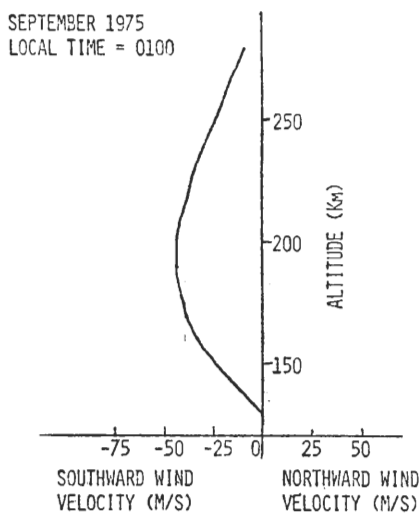


Fig. 15. Computed vertical wind profiles of meridional component and zonal component at 0100 local time, September 1975.

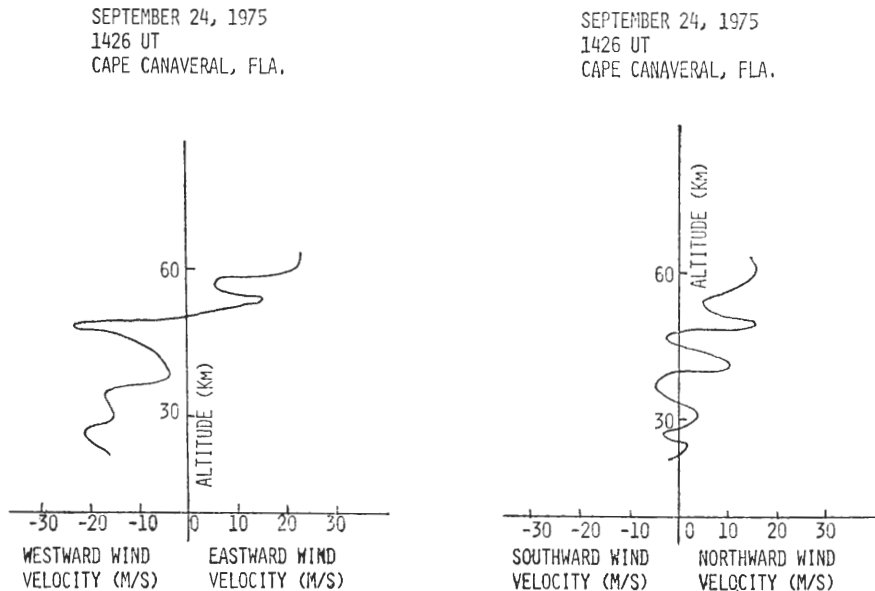


Fig. 16. Observed vertical wind profiles of meridional and zonal components from meteorological rocketsonde data at 1426 UT, September 24, 1975, at Cape Kennedy, Florida.

#### 4. Sources of the Waves

(A) **Tornadic Storms.** The time period of the observation for the present tornadic storm cases of April 3, 1974 was from 12:00 a. m. to 5:00 p. m. local time. During this time period, the electron density distribution was rather stable and the radio wave reflection height with a frequency of 4.0125 MHz was around 240 km. Thus, the reverse ray tracing is started at an altitude of 240 km and continues as long as the calculation is possible to a lower limit of 10 km altitude. For the purpose of the present study the geographic location of the point at which the calculation is terminated is referred to as the probable source. The probable sources of the gravity waves are then checked with the actual physical features, which is the computer printout of locations and times of tornado touchdowns supplied by the National Severe Storms Forecast Center (hereafter NSSFC).

Fig. 17 shows trajectories of the computer reverse group ray paths for the waves observed in terms of height against horizontal distance. The group ray paths in the horizontal distance are again projected in the maps to show the geographic locations of the probable sources of the waves.

Fig. 18 shows the horizontal ray path and the geographical location of the probable source of the wave which was detected in the ionospheric height with receivers at Huntsville, Alabama, at 1700–1800 UT, April 3, 1974. The tornado touchdown data supplied by NSSFC indicated that, within 50 km radius from the probable source of waves, there were two tornado touchdowns; one at 1930 UT, and the other at 2030 UT. The actual traveling time of the gravity waves from the probable source to Huntsville, Alabama took 64 minutes. In other words, the signal was excited roughly 3 hours and 30 minutes ahead of the touchdown of tornadoes.

The geographical location of the probable source of the wave detected at 1800–1900 UT, April 3, 1974, is presented in Fig. 19. Within 20 km distance from the computed probable source of the wave, the tornado touchdown data supplied by NSSFC indicated that there was a tornado touchdown at 2100 UT. The actual wave traveling time from the probable source to the receivers at Huntsville, Alabama took 43 minutes. Thus, in this case, the signal was generated roughly 3 hours and 40 minutes ahead of the touchdown of the tornadoes.

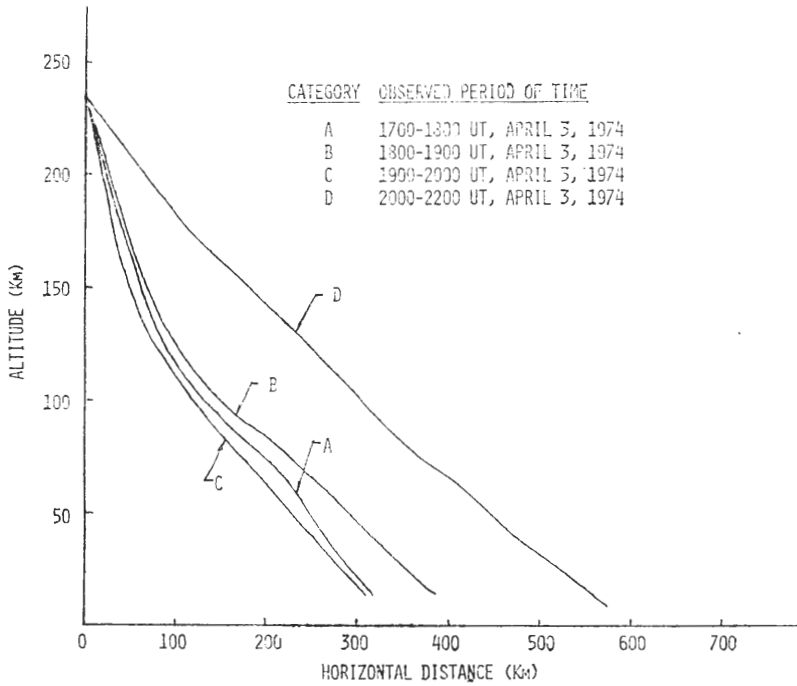


Fig. 17. Trajectories of the computed reverse group ray path for the waves in the time periods 1700-1800, 1800-1900, 1900-2000, and 2000-2200 UT, April 3, 1974, in terms of height against horizontal distance.

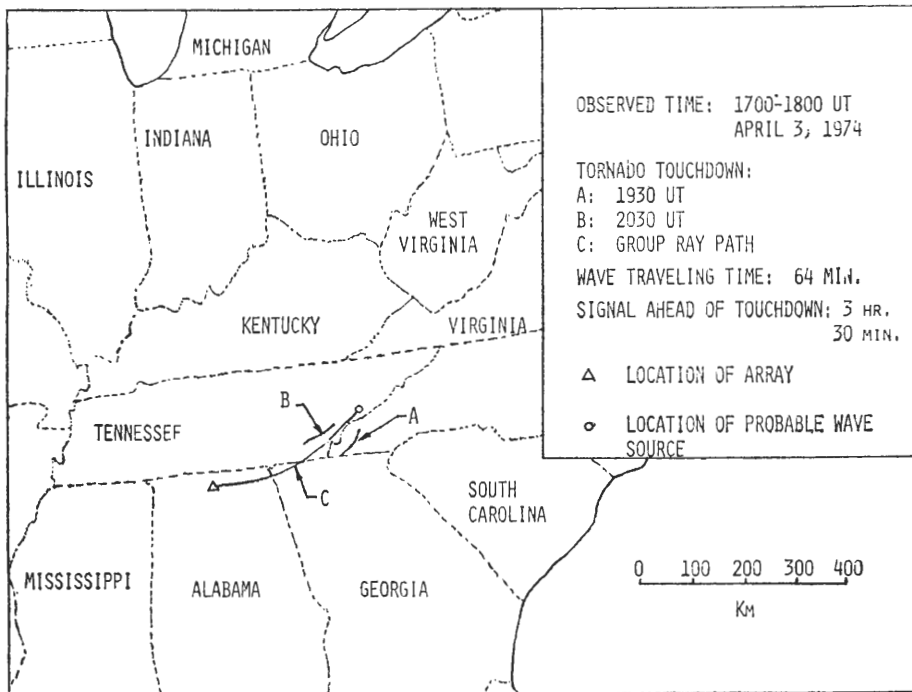


Fig. 18. Geographical map of the trajectory of the computed group ray path of waves during the time period 1700-1800 UT, April 3, 1974, and the location and time of actual tornado touchdown.

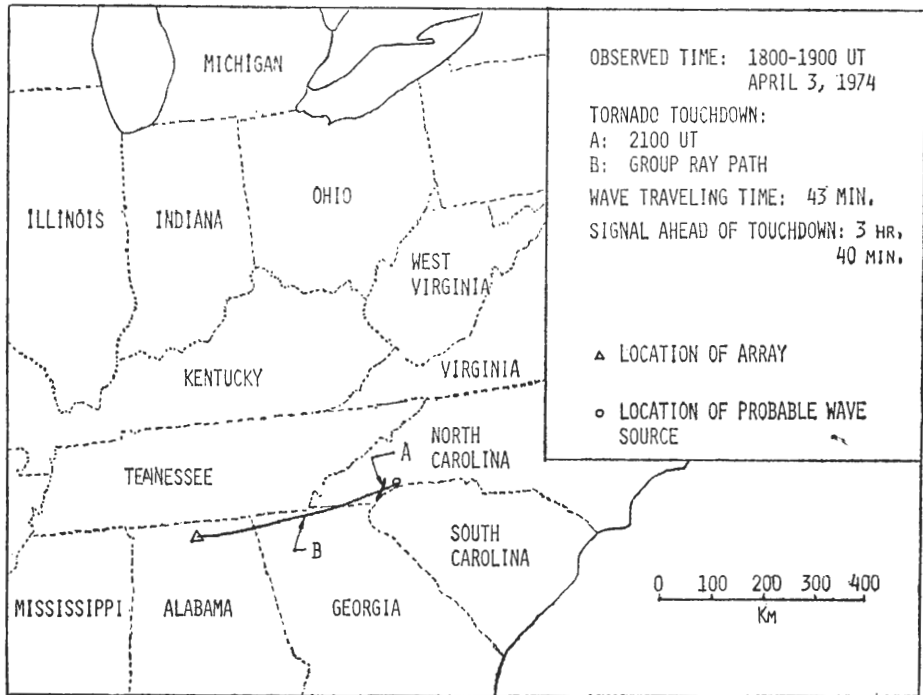


Fig. 19. Geographical map of the trajectory of the computed group ray path of waves during the time period 1800-1900 UT, April 3, 1974, and the location and time of actual tornado touchdown.

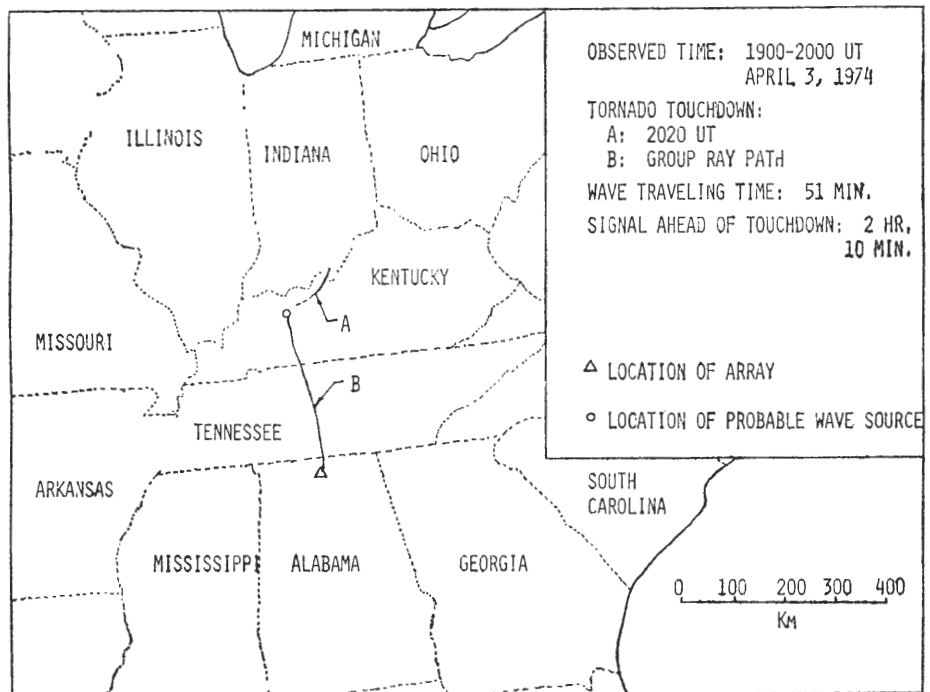


Fig. 20. Geographical map of the trajectory of the computed group ray path of waves during the time period 1900-2000 UT, April 3, 1974, and the location and time of actual tornado touchdown.

Fig. 20 shows another geographical location of the probable source of the wave which was detected in Huntsville, Alabama at 1900–2000 UT, April 3, 1974. NSSFC data indicated that the tornado touched down at 2020 UT, within 15 km distance from the computed probable source of the wave. The actual wave traveling time from this probable source to Huntsville, Alabama was 51 minutes. This indicates that the signal was excited approximately 2 hours and 10 minutes ahead of the touchdown of the tornado.

The geographical location presented in Fig. 21 indicates the horizontal ray path of the wave which was detected in Huntsville, Alabama at 2000–2200 UT, April 3, 1974. NSSFC data pointed out that a series of tornadoes touched down at 2125, 2130 and 2145 UT within 50 km distance from the computed probable source of the waves. In this case, the actual wave traveling time from the probable source of the wave to the receivers at Huntsville, Alabama was 1 hour 52 minutes. In other words, the signal was excited roughly 3 hours and 10 minutes ahead of the touchdown of the torna-

does.

(B) **Hurricane.** The observation time for Hurricane Eloise was 0200–0730 UT, September 23, 1975. The corresponding radio wave reflection height with a frequency of 4.0125 MHz was around 270 km. Thus, the reverse ray tracing is started at an altitude of 270 km and continues as long as the calculation is possible to the lower altitude near the ground. This geographic location of the point at which the calculation is terminated is referred to as the probable sources of waves. The probable sources of gravity waves are then checked with the actual storm track of the hurricane.

Fig. 22 shows trajectory of the computer reverse ray path for the waves observed during the time period 0200–0340 UT, September 23, 1975, in terms of height against horizontal distance. Fig. 23 shows another trajectory of the computer reverse ray path observed during the time period 0500–0730 UT, September 23, 1975 for the similar profile. Again, the group ray paths in the horizontal distance are projected in the map to show the geographical location of the probable sources of waves.

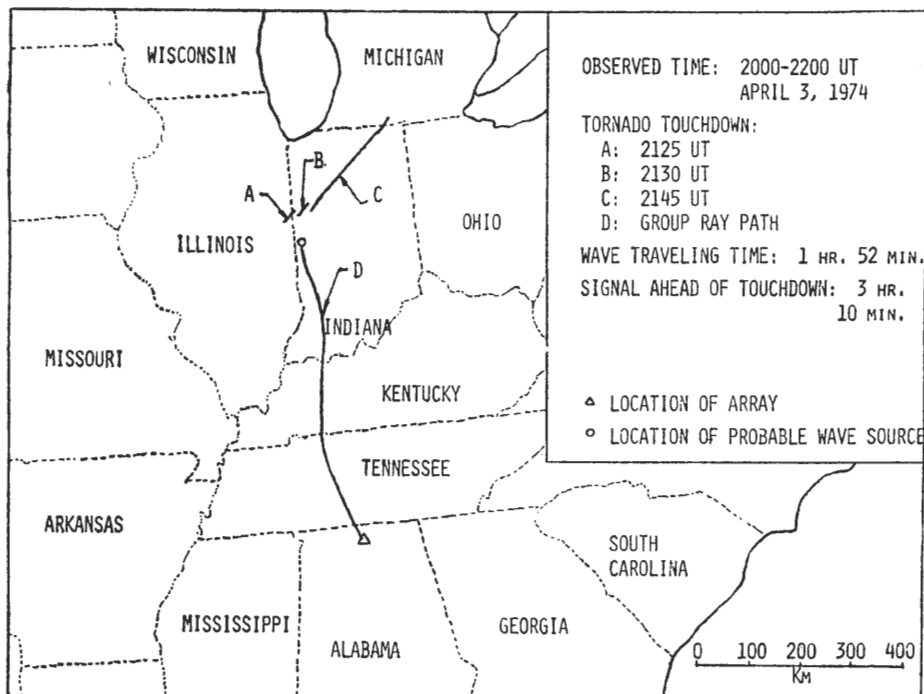


Fig. 21. Geographical map of the trajectory of the computed group ray path of waves during the time period 2000–2200 UT, April 3, 1974, and the location and time of actual tornado touchdown.

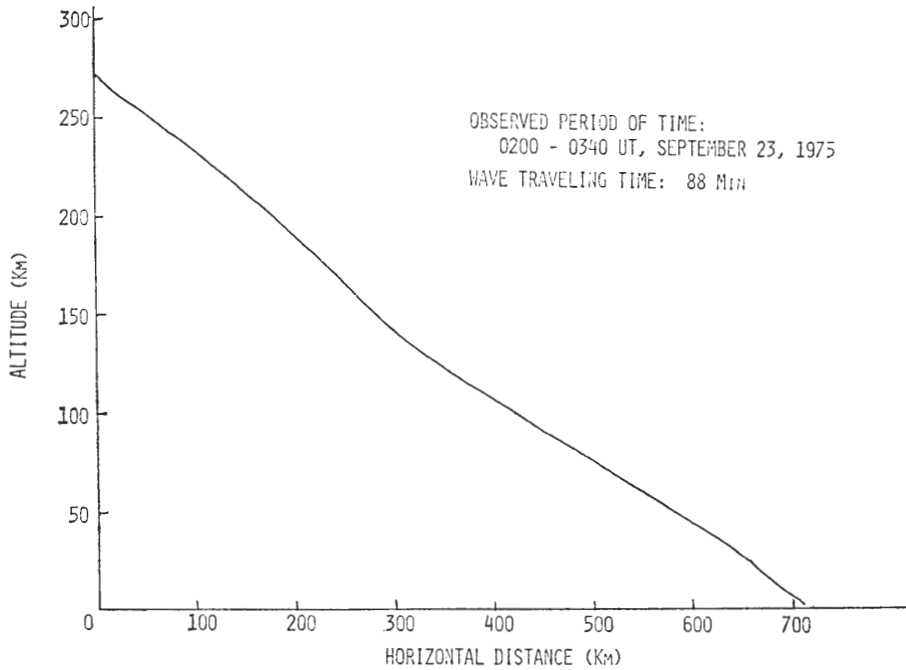


Fig. 22. Trajectory of the computed reverse group ray path for the waves during the time period 0200-0340 UT, September 23, 1975, in terms of height against horizontal distance.

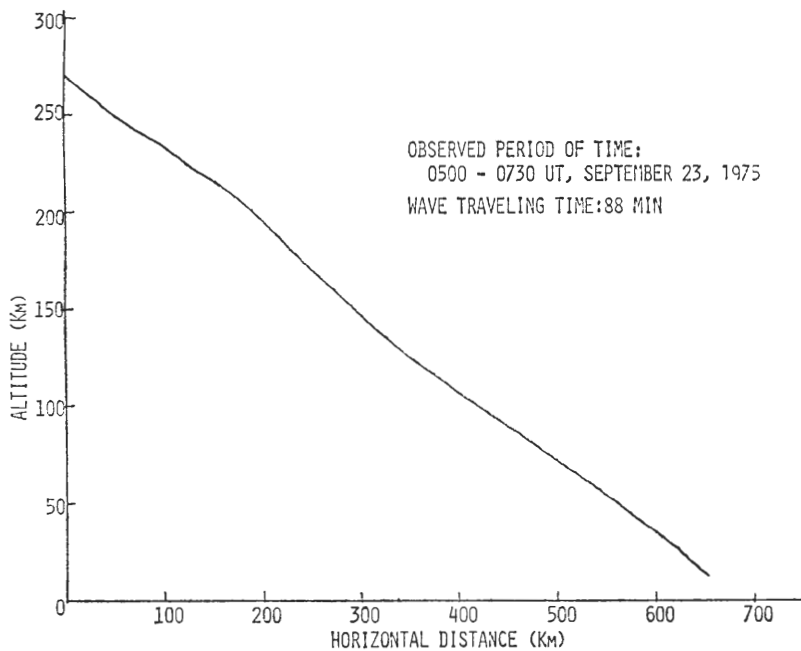


Fig. 23. Trajectory of the computed reverse group ray path for the waves during the time period 0500-0730 UT, September 23, 1975, in terms of height against horizontal distance.

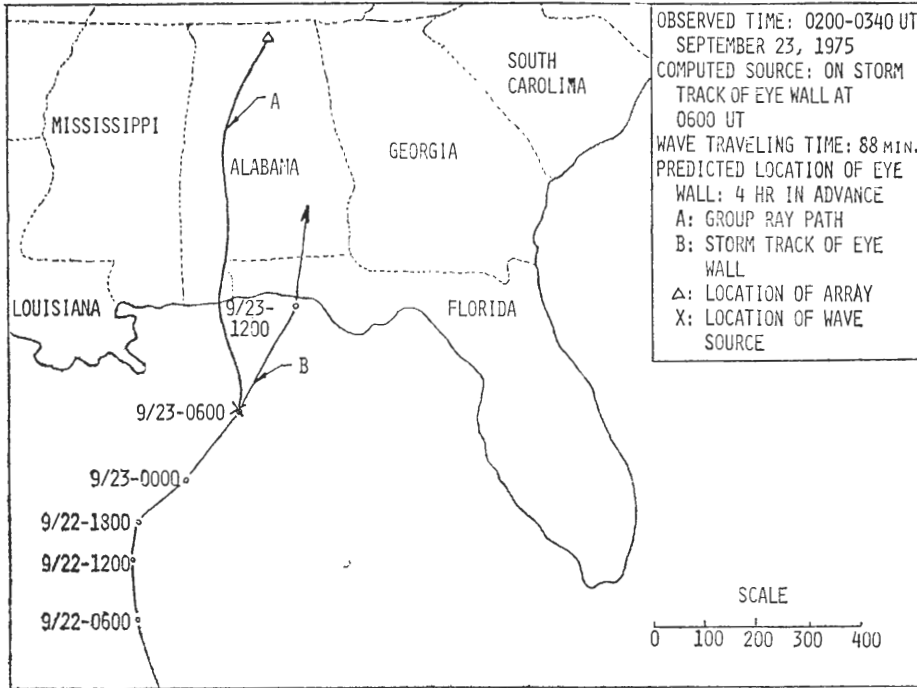


Fig. 24. Geographical map of the trajectory of the computed group ray path of waves during the time period 0200-0340 UT, September 23, 1975, and storm track of the eye wall of Hurricane Eloise.

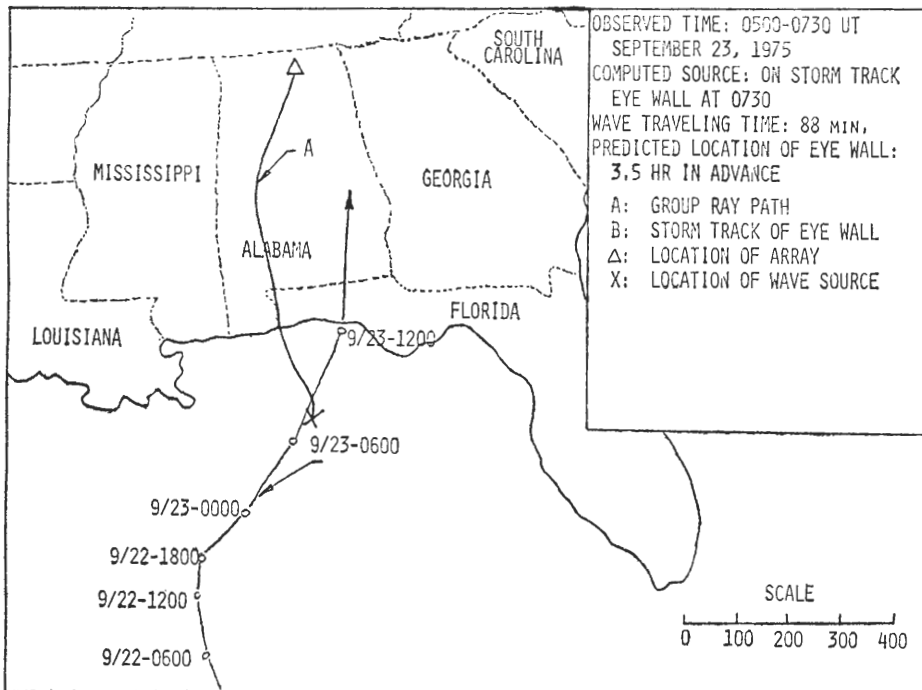


Fig. 25. Geographical map of the trajectory of the computed group ray path of waves during the time period 0500-0730 UT, September 23, 1975, and storm track of the eye wall of Hurricane Eloise.

Fig. 24 shows the horizontal ray path and the geographical location of the probable source of the wave which was detected in the ionospheric height with receivers at Huntsville, Alabama, at 0200-0340 UT, September 23, 1975. The computed location of the wave source is located right on the storm track of the eye wall at 0600 UT, September 23, 1975. The calculated traveling time of this wave from the probable source to the receiver at Huntsville, Alabama was 88 minutes. Thus, in this particular case, the location of the eye wall of the hurricane could have been predicted roughly 4 hours in advance.

Fig. 25 shows another geographical location of the probable source of the wave which was observed at 0500-0730 UT, September 23, 1975. In this case, the computed probable source of the wave is located right on the storm track of the eye wall at 0730 UT, September 23, 1975. The calculated traveling time of this wave from the probable source to the receiver at Huntsville, Alabama was also 88 minutes. Thus, the location of the eye wall of the hurricane is predictable approximately 3.5 hours in advance.

## 5. Discussions and Conclusions

During the time period of the extreme tornado outbreak of April 3, 1974, wave-like

disturbances were observed on ground-based ionospheric sounding records as perturbations in electron densities. Four events of the observations indicate that gravity waves with wave periods of 13 to 28 minutes (mostly around 13 minutes) and wavelengths from 100 to 170 km were detected at the *F*-region ionospheric height during the tornado activity. A group ray path computation has been applied to trace the gravity waves observed at ionospheric height and effort is made to compute the probable source of the waves. A comparison of the results of the computed probable source of waves and the location and time of the tornado touchdown supplied by the National Severe Storms Forecast Center, Kansas City, Missouri, clearly indicated that the locations of the tornado touchdown were within 50 km or less distance from the computed location of the probable sources of waves. Table 1 shows the four events of propagation characteristics of the observed waves and comparisons with tornado touchdown data. More significantly, the signals-excited by the storms were 2 to 4 hours ahead of the touchdown of the tornadoes in the present study.

Similar observations of wave-like disturbances were also concluded when the eye wall of Hurricane Eloise was located at the Gulf of

Table 1. Propagation Characteristics of the Observed Waves and Comparison with Tornado Touchdown Data Supplied by the National Severe Storms Forecast Center, Kansas City, Missouri, on April 3, 1974.

Observed Time (UT)	Wave Period (minutes)	Horizontal Wavelength (km)	Azimuth Angle of Wave Vector (deg)	Horizontal Phase Speed (m/sec)	Wave Traveling Time (min)
1800-1900	13	169	255	217	43
1900-2000	13.5	129	146	160	51
2000-2200	28	150	179	90	112

Observed Time (UT)	Tornado Touchdown Time (UT)	Distance Between Computed Wave Source and Touchdown Location (km)	Signal-Excited Ahead of Tornado Touchdown	
			hr	min
1700-1800	1930	50	3	30
1800-1900	2100	20	3	40
1900-2000	2020	20	2	10
2000-2200	2125	50	3	10



Mexico. During this time period gravity waves with wave periods of 21 to 25 minutes and horizontal phase velocities of 110 to 210 m/sec were detected. The results from group ray tracing computation indicated that the computed probable source of the waves was located right on the storm track of the eye wall and was 3 to 4 hours in advance for the present study of the case of Hurricane Eloise.

It is known that mesoscale behavior causes severe weather and disruptive, violent storms. Mesoscale motions are inherently only predictable for short times, but even a few hours warning of severe weather can be of value (Suomi, 1975). The results from the present study indicate that tornadoes could be predicted 2 to 4 hours ahead of the touchdown, and hurricane tracks could also be predicted 3 to 4 hours in advance, if the observation stations are properly distributed and the analysis is accomplished in real time.

The accuracy and reliability of the group ray path computation could be improved if the systematic measurements of the winds from the ground to the ionospheric height, in particular from 20 to 100 km altitudes, are accomplished. In the present study, for the neutral wind velocities above 100 km altitude, the profiles are obtained by using the method of computing the wind model proposed by Kohl and King (1967); and for the neutral wind velocities below 100 km, the profiles are based on meteorological rocketsonde data measured at Cape Kennedy, Florida, which is 1000 km away from the location of our receivers. The improvement of the accuracy of the wind profiles in any respect other than the current situations will certainly increase the reliability of tracing the path of infrasonic-gravity waves excited by severe storms.

**Acknowledgment:** The computer computation accomplished by T. Phan and J. P. Kuo is appreciated. The author appreciates the support of the present research from the National Science Foundation/U. S. Army Research Office through a grant NSF/ATM 75-15706, and also the Division of International Programs of the

National Science Foundation through the grant NSF/INT 76-00745.

#### REFERENCES

- BAKER, D. M. and K. DAVIES, 1969: F2-Region acoustic waves from severe weather. *J. Atmos. Terr. Phys.*, **31**, 1345-1352.
- BERTIN, F., J. TESTUD, and L. KERSLEY, 1975: Medium scale gravity waves in the ionospheric F-region and their possible origin in weather disturbances. *Planet. Space Sci.* **23**, 493-501.
- BRETHERTON, F. P., 1966: The propagation of groups of internal gravity waves in a shear flow. *Quart. J. Roy. Meteor. Soc.*, **92**, 466-480.
- COWLING, D. H., H. D. WEBB, and K. C. YEH, 1971: Group rays of internal gravity waves in a wind stratified atmosphere. *J. Geophys. Res.*, **76**, 213-220.
- DAVIES, K. and J. E. JONES, 1972: Ionospheric disturbances produced by severe thunderstorms. NOAA Professional Paper 6, U. S. Dept. of Commerce, NOAA, Rockville, Md., pp. 47.
- GEORGES, T. M., 1968: Short-period ionospheric oscillations associated with severe weather. *Proc. Symp. Acoustic-Gravity Waves in the Atmosphere*, Govt. Printing Office, Washington, D. C., 171-178.
- HINES, C. O., 1960: Internal atmospheric gravity waves at ionospheric heights. *Can. J. Phys.*, **38**, 1441-1481.
- HUNG, R. J., R. E. SMITH, G. S. WEST and B. B. HENSON, 1975: Detection of upper atmospheric disturbances in northern Alabama during extreme tornado outbreak of April 3, 1974. *Ninth Conference on Severe Local Storms*. Amer. Meteor. Soc., Boston, Mass., 294-300.
- JONES, W. L., 1969: Ray tracing for internal gravity waves. *J. Geophys. Res.*, **74**, 2028-2033.
- KOHL, H. and J. W. KING, 1967: Atmospheric winds between 100 and 700 km and their effects on the ionosphere. *J. Atmos. Terr. Phys.*, **29**, 1045-1062.
- SMITH, R. E. and R. J. HUNG, 1975: Observation of severe weather activities by Doppler sounder array. *J. Appl. Meteor.* **14**, 1611-1615.
- SUOMI, V. E., 1975: Atmospheric research for the nation's energy program. *Bull. Amer. Meteor. Soc.*, **56**, 1060-1076.
- U. S. Standard Atmosphere, 1962: Govt. Printing Office, Washington, D. C., 1-278.
- YEH, K. C. and C. H. LIU, 1972: *The Theory of Ionospheric Waves*, Academic Press, New York, pp. 464.

# 利用重力波徵兆特性以預報颱風及龍捲風

洪 儒 珍

美國阿拉巴馬大學亨滋維校區

## 摘 要

由地面觀測電離層之下層區域發現在颱風期間有周期 21 至 25 分鐘及水平位相速度 110 至 210 米/秒之重力波，在龍捲風期間則有周期 13 至 28 分鐘（大都在 13 分鐘左右）及水平位相速度 90 至 220 米/秒之重力波。利用中性大氣及中性風縱斷面之數據，我們可以用羣波段追蹤法來計算波源之位置。比較所計算之波源位置與颱風之位置發現波源位置在颱風眼 3 至 4 小時後的未來位置上。至於龍捲風則所計算之波源位置在龍捲風觸地前 2 至 4 小時之位置上。利用重力波徵兆之特性在惡劣天候預報作業上之可能應用亦將詳細討論。

## Appendix A

Consider two time series functions given by  $X_\alpha(t)$  and  $X_\beta(t)$ . The cross-correlation function is given by

$$C_{\alpha\beta}(t) = \lim_{T \rightarrow \infty} \frac{1}{2T} \int_{-T}^T X_\alpha(t) X_\beta(t + \tau) d\tau$$

where  $\tau$  is the time lag, or the time displacement between the two functions being correlated. In a special case when  $X_\alpha = X_\beta$ ,  $C_{\alpha\alpha}$  becomes the auto-correlation function

$$C_{\alpha\alpha}(t) = \lim_{T \rightarrow \infty} \frac{1}{2T} \int_{-T}^T X_\alpha(t) X_\alpha(t + \tau) dt$$

The power spectral density and cross power spectral density are obtained by Fourier trans-

forming the auto and cross correlation functions, respectively, i. e.,

$$P_{\alpha\alpha}(\omega) = \frac{1}{2\pi} \int_{-\infty}^{\infty} C_{\alpha\alpha}(\tau) e^{-i\omega\tau} d\tau$$

and

$$P_{\alpha\beta}(\omega) = \frac{1}{2\pi} \int_{-\infty}^{\infty} C_{\alpha\beta}(\tau) e^{-i\omega\tau} d\tau$$

where  $\omega = 2\pi f$  is the angular frequency in radian/sec and  $f$  is frequency in Hz. The power spectral density with maximum spectral density normalized by unity is termed normalized power spectral density, while the power spectral density without normalization is called relative power spectral density.